Analysis of refrigerants flow inside an adiabatic spirally coiled capillary tube

Abdullah A. A.A. Al-Rashed
Public Authority for Applied Education and Training, Industrial Training Institute, 13092 *Kuwait*

Air-conditioners use spirally coiled capillary tubes as an expansion device to enhance compactness of the unit. However, most empirical correlations for predicting refrigerant flow rate through capillary tubes were developed for straight capillary tubes without consideration of coiled effects. The objectives of this study are to investigate the flow characteristics of the coiled capillary tubes and to develop a generalized correlation for the mass flow rate through the coiled capillary tubes. The mass flow rate of R22 through the coiled capillary tubes and straight capillary tubes was measured for various operating conditions and tube geometries. The mass flow rates of the coiled capillary tubes less by 5–16% than those of the straight capillary tubes at the same operating conditions. A generalized correlation for predicting refrigerant mass flow rate through coiled capillary tubes was developed by introducing the parameter of capillary equivalent length .This paper presents an experimental investigation for the flow of R-134a inside an adiabatic spirally coiled capillary tube. The effect of various geometric parameters like capillary tube diameter, length and coil pitch for different capillary tube inlet sub-cooling on the mass flow rate of R-134a through the spiral capillary tube geometry has been investigated. It has been established that the coil pitch significantly influences the mass flow rate of R-134a through the adiabatic spiral capillary tube. The effect of providing pressure taps on the capillary tube surface has a negligible effect on the mass flow rate through the capillary tube. The data obtained from the experiments are analyzed and a semi-empirical correlation has been developed. The proposed correlation predicts more than 91% of the mass flow rate which is in agreement with measured data in an error band of ±10%.

يتم استخدام الانابيب الشعرية الملفوفة بشكل حلزوني في مكيفات الهواء، بوصفها اداة لتعزيز توسع الاكتناز للوحدة. و مع ذلك فإن معظم الإرتباطات التجريبية لتنبؤ المبردات بمعدل التدفق من خلال الانابيب الشعرية وضعت دون النظر في آثار درجة ألتفاف تلك الانابيب و طرق تصميمها. تهدف هذه الدراسة الي التحقيق في خصائص تلك الانابيب الملفوفة بشكل حلزوني ودرجة ارتباط معدل تدفق سائل التبريد من خلال تلك الانابيب. و من خلال نتائج تلك الدراسة تم التوصل الي ان اثر اللف في الانبوب الشعري يقلل من معدل التدفق بنسبة ٥-١٥%، بالمقارنة مع انابيب مباشرة تعمل تحت ظروف مماثلة. كما ان معدل تدفق سائل التبريد R-22 يقل بنسبة ٥-١٦% في حالة استخدام انابيب مستوية و غير ملفوفة بشكل حلزوني.

Keywords: R-134a, Refrigerant, Capillary, Flow, Correlation

1. Introduction

A capillary tube has been used as an expansion device in small refrigeration and air-conditioning systems. It controls the refrigerant mass flow and balances the system pressure in the refrigeration cycle. It is simple and low cost and has a low starting torque. Generally, refrigeration systems use a spirally coiled capillary tube to construct a compact unit. The shape of the coiled capillary tube can considerably affect the mass flow rate in the refrigeration cycle because the flow resistance from the secondary flow varies with the coiled shape H. Ito, Friction factors for turbulent flow in curved pipes, *J. Basic Eng.* (1959), pp. 123–134. Capillary tubes are being used as an expansion device in the low capacity refrigerating machines like domestic refrigerators and window type room air conditioners. These are narrow drawn copper tubes of 0.5–2.0 mm bore and 2–6 m length. Owing to the simplicity, low cost, zero maintenance and requirement of a low starting torque motor to run the compressor, capillary tubes have been used in a variety of vapor compression systems. The various flow aspects of the capillary tube were investigated by a number of researchers since past six decades. Bolstad and Jordan (1948) pioneered the investigations on capillary tubes. They studied the effect of oil entrainment on the

mass flow rate through the capillary tube. It was found that the use of oil separator in the system decreases the flow rate by 8% in comparison to that when no oil separator was used. Mikol (1963) carried out an extensive experimental investigation on the capillary tube to explore the various flow phenomena like metastability and choking. They developed a friction factor correlation by flowing water through the same capillary tube.

The effects of coiling on the refrigerant mass flow rate of the refrigerant had been discussed by a few investigators. Kuehl and Goldschmidt (1990) have conducted experiments on the flow of R-22 through adiabatic capillary tubes of straight and coiled geometries. They have concluded that because of the coiling of capillary tube, the refrigerant mass flow rate was reduced by not more than 5%. Kim et al. (2002) have studied the flow of R-22 and its alternatives, viz., R-407C and R-410A through the straight and helically coiled adiabatic capillary tubes. They have observed 9% reduction in refrigerant mass flow rate through a coiled tube in comparison to that in straight tube of same length. Zhou and Zhang (2006a) conducted an experimental investigation on helically coiled capillary tubes for the flow of refrigerant R-22. In addition, a numerical model using Mori and Nakayama friction factor correlation (Mori and Nakayama, 1967) was also proposed. It was concluded that for the mean coil diameter beyond 300 mm, the change in mass flow rate was insignificant. It was also observed that the refrigerant mass flow rate through a helical capillary tube with coil diameter of 40 mm was approximately 10% less than that of the straight capillary tube. Further, Zhou and Zhang (2006b) confirmed the hysteresis in refrigerant mass flow rate with increasing and decreasing inlet sub-cooling in an adiabatic helical capillary tube. The hysteresis effect was more prominent in helical capillary tube than that in straight tube due to the disturbance generated from the secondary flows caused by the centrifugal force. It was also found that in the coiled capillary tube the refrigerant flashed earlier with decreased coil diameter as reduction in coil diameter caused the pressure drop to increase. However, for validation of the numerical model with the experimental data, the increasing sub-cooling data should be taken into account due to their consistency and reproducibility. A recently published literature on coiled adiabatic capillary by Park et al. (2007) for the flow of R-22 and its alternatives, R-407C and R-410A, has revealed a slightly higher drop in mass flow rates of the coiled capillary tubes compared to those in straight capillary tubes as reported by Kim et al. (2002) and Zhou and Zhang (2006a). It was found by Park et al. (2007) that the mass flow rate of the coiled capillary tubes was decreased by 5–16% in comparison to that for the straight capillary tubes. They also proposed a generalized mass flow rate correlation for helically coiled capillary tubes based on Buckingham-π theorem. In addition, a numerical model based on homogenous two-phase flow model was presented using Ito (1959) friction factor correlation for single phase flow and Giri's equation for two-phase flow (Gorasia et al., 1991). Valladares (2007) also presented a numerical simulation model for the coiled capillary tubes based on the finite volume formulation. The solution was carried out using an implicit step-by-step numerical scheme. The calculation of mass flow rate was made iteratively using Newton–Raphson Algorithm.

The experimental studies on spiral capillary tubes are not available in the literature. However, only Khan et al. (2007) have proposed a numerical model for the computation of length of adiabatic spiral capillary tube. It has been found that because of coiling the length of the capillary tube are reduced considerably for a given set of input conditions.

Previous researchers have also proposed a number of correlations to predict the refrigerant flow rate for a given capillary tube. For instance, correlations for the mass flow rate of different refrigerants proposed by Wolf et al. (1995) are available in ASHRAE Handbook (2006). Another important study regarding the flow of newer refrigerants inside capillary tubes has been carried out by Melo et al. (1999). They proposed separate correlations for R-12, R-134a and R-600a and a combined mass flow rate correlation for all three refrigerants for the flow inside an

adiabatic capillary tube. Choi et al. (2003) have proposed new dimensionless parameters and developed a correlation for the prediction of mass flow rate through the capillary tubes.
Since, experimental data for the flow of R-134a refrigerants through spiral capillary tube are not available in the literature, an experimental investigation has been undertaken to study the flow of R-134a through a spiral capillary tube.

2. Experimental set-up and procedure

The schematic diagram of a experimental set-up has been shown in Fig. 1. The test-section (1) was a copper capillary tube, in which the refrigerant expands from high pressure side to low pressure side. The spirally coiled tube's test-section in the experimental apparatus was put in horizontal position. From capillary tube refrigerant entered the evaporator (2) consisting of a copper coil submerged in a water tank. A 5.0 kW capacity electric heater (3) was fitted in the evaporator tank to provide heat load to evaporator. The heating load was varied through a variac (4). An agitator (5) was also provided in the tank to maintain the uniform bulk temperature of water. The vapors emerging from the evaporator were sent to liquid accumulator (6) in order to avoid liquid refrigerant to enter the compressor (7). The compressor (7) was run by means of three phase electric motor (8) using belt and pulley type arrangement. The high pressure superheated vapors emerging from the compressor entered through the oil separator (9). After several trial runs, the visual inspection from the sight glass revealed no trace of oil. As an additional check, the capillary tube was tear open and the inside surface was rubbed with white absorbent paper. The oil free vapors from separator (9) were condensed in the water cooled condenser (10). The cooling water was circulated in the condenser by means of a centrifugal pump (11). The high pressure saturated liquid from condenser was collected in a receiver (12) to ensure a continuous supply of refrigerant to the capillary tube. The unwanted solid particles and moisture in refrigerant were removed through drier-cum-filter (13). The bank of four rotameters (14) with one digital rotameter (DR) and three float type rotameters (R1, R2 and R3) of different ranges was installed after the drier-cum-filter. The mass flow rate data have been acquired by digital rotameter (DR) whereas other three rotameters were placed in parallel to cross verify the mass flow rate measured by digital rotameter. A refrigerant subcooler (15) was provided after the rotameters. The chilled water to the subcooler was supplied by means of a separate chiller unit based on the vapour compression cycle with R-22 as a working fluid. The chiller consisted of a hermetically sealed compressor (16), an air cooled condenser (17), and a tank for cooling water. A centrifugal pump (18) was used to circulate chilled water through the subcooler (15). To vary the degree of subcooling at the capillary tube inlet, a preheater (19) followed the subcooler (15). In the preheater, resistance heating of tube carrying the refrigerant was done and the heat input was controlled by a variac (20). A sight glass (21) was provided after the preheater to visualize the state of refrigerant flow. A hand operated expansion valve (22) was also provided after the condenser (10) to control the refrigerant flow rate in capillary tube by bypassing the excess refrigerant. A number of hand shut-off valves (23) were provided in between the major components of the experimental set-up, in case of leak or repair; the damaged component could be retrieved with ease. The temperature at different locations of the set-up and the test-section was measured by means of copper–constantan (T-type) thermocouples (24) while the pressure of the refrigerant was measured with pressure gauges (26) as well as pressure transducers (27) using pressure headers (25). A total of four pressure headers were used in the set-up of which three are shown in fig. 1. Further, the pressure at the suction and discharge of the compressor were measured with separate bourdon tube (commercial) pressure gauges.

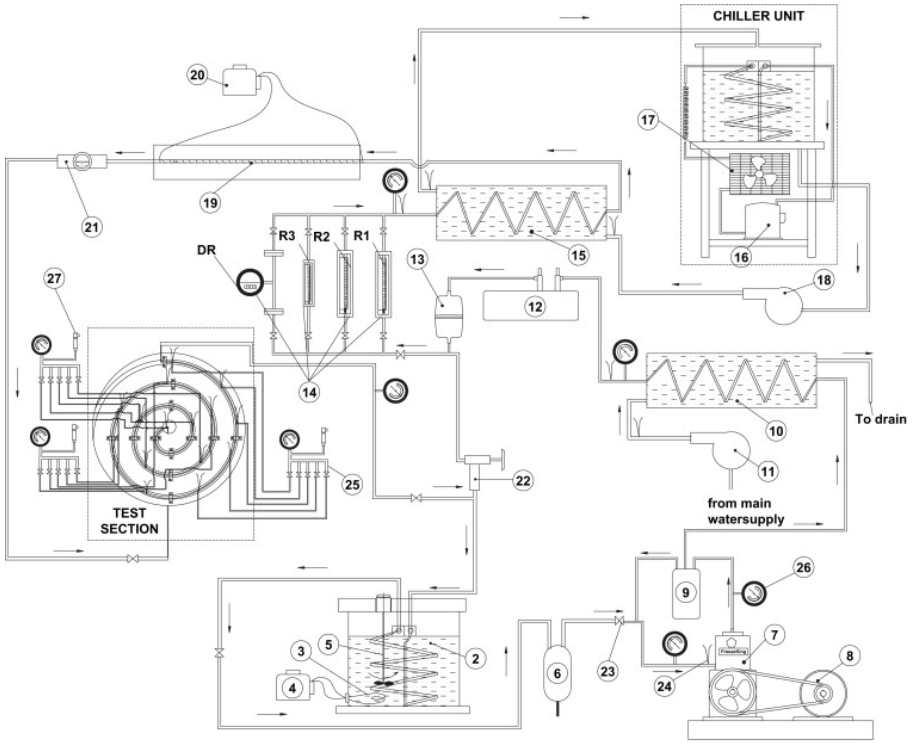

Fig. 1. Experimental set-up layout.

Spiral tube test-section was formed by first producing spiral groove of required pitch on the face of the wooden discs of 600 mm in diameter and 50 mm thickness. Making of a spiral required two points 'c_1' and 'c_2' offset by a distance of 'x' mm. With the help of a compass, a semicircle of 'x' mm radius was drawn taking 'c_1' as centre and another inverted semicircle of twice the offset distance (i.e., $2x$) taking 'c_2' as centre. The above procedure was repeated till the curve reached the disc periphery. The step-by-step procedure of generating spiral has been shown in fig. 2-a.

The relation between the offset distance and the pitch of spiral is as follows:

$$p=3x. \quad (1)$$

Once the spiral was marked on the disc, with the help of mortise chisel a groove large enough to accommodate the capillary tube of 1.63 mm (ID) was carved out of the disc. The process of carving out of spiral required high degree of workmanship. Fig. 2-b shows three wooden discs having spiral grooves of three different pitches, viz., 20 mm, 40 mm and 60 mm. A hole of 25 mm size was drilled at the centre of the each disc so as to facilitate the capillary tube to pass through the disc. The test-section was insulated by putting a thick layer of ceramic wool on the test-section. Moreover, an aluminum sheet was fixed around the periphery to house the ceramic wool insulation. The final arrangement of spiral test-section has been shown in fig. 3. Three pitches for three capillary tube diameters were used to investigate the flow of R-134a inside the spirally coiled geometry of capillary tube. Three different wooden circular discs of 600 mm diameter were used for different coil pitches. To elaborate it further,

the capillary tube of a given diameter and length 6.4 m was taken. In order to measure the pressure along the capillary tube, 15 taps at a gap of 40 mm have been provided on the length of capillary tube. 'T-joint', also shown in Fig. 3, was brazed on the capillary tube to house the aperture on the capillary tube surface. Then, the capillary tube with T-joints brazed over the taps was fixed in the spiral groove of the given wooden cylindrical disc by means of a number of clips. The fabrication of 'T-joint' required good workmanship as during brazing of T-joint a controlled heating of the tapped zone was required otherwise tube was blocked. And it is because of this the brazing was done a distance away from the aperture using T-joints. The aperture or pressure tap is produced by weakening the wall of capillary tube by a smooth round file. The weakened zone was subjected to piercing by the sharp tip of a needle. The process described for generating pressure taps was first employed by Bolstad and Jordan (1948). Instead of piercing the capillary tube, they employed drilling operation to produce the hole on the capillary surface. The tap diameter as measured by microscope was approximately 0.25 mm with an accuracy of 0.01 mm.

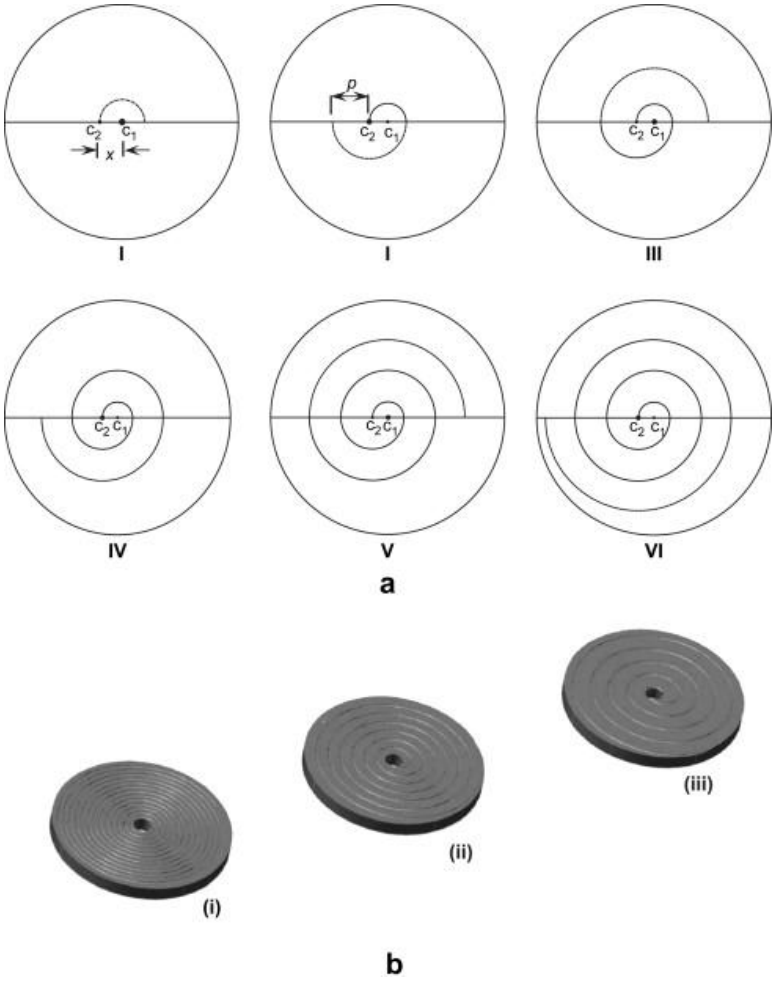

Fig. 2-a Step-by-step procedure for generating spiral. B- Spiral patterns for three pitches: (i) 20 mm (ii) 40 mm, and (iii) 60 mm.

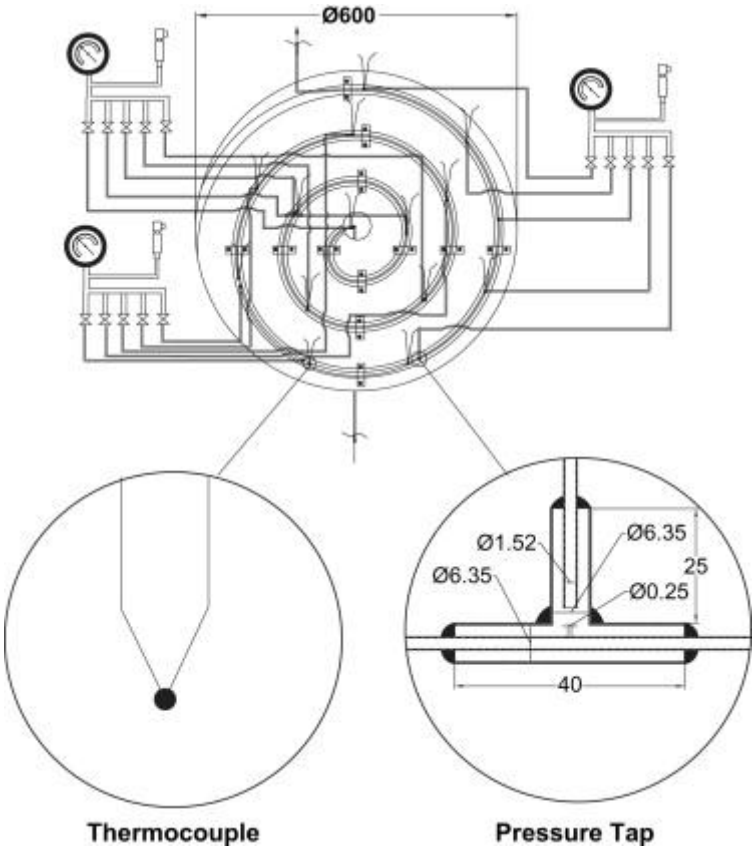

Fig. 3. Schematic diagram of the test-section.

The capillary tube with pressure taps generated on its surface was termed as instrumented capillary tube while the tube without pressure taps was known as non-instrumented capillary tube. A total of 14 test-sections were used in the present experimental study, the details of capillary tube and range of operating parameters have been shown in table 1. For spiral geometry nine instrumented test-sections and one non-instrumented test-section of 1.4 mm capillary diameter and 40 mm coil pitch whereas for straight geometry three instrumented test-sections and one non-instrumented test-section of 1.4 mm capillary tube diameter were used in the present experimental investigation.

Initially, the capillary tube of a given diameter and length 6.4 m was taken. A total of six lengths for each test-section were investigated. Each length is obtained by cutting the capillary tube by 0.8 m. For each length, the degree of subcooling at the capillary tube inlet was controlled by the subcooler and the preheater together. For a particular capillary length, 4–5 subcoolings were obtained in the range of 0–20 °C. The mass flow rate corresponding to each level of inlet subcooling was recorded. The pressure at capillary inlet for all experimental runs was maintained constant at 740 kPa.

The internal surface roughness of the capillary tubes was measured using Surface Profilometer. For the measurement of surface roughness, a piece of capillary tube was sliced into two halves. The roughness for the capillary tubes of diameters 1.12 mm, 1.40 mm and 1.63 mm was found to be 7.05 μm, 6.22 μm and 3.58 μm, respectively. The capillary tube diameters and the pressure tap diameters were measured with the help of Tool maker's microscope. The internal diameters of the capillary tubes are 1.12 mm, 1.40 mm and 1.63 mm, respectively.

Table 1
Range of input parameters

Parameters	Selected range			
	Straight capillary tube		Spiral capillary tube	
	Instrumented	Non-instrumented	Instrumented	Non-instrumented
d (mm)	1.12, 1.40, 1.63	1.35	1.14, 1.47, 1.63	1.40
L (m)[a]	6.2–2.3			
e/d	0.0053, 0.0064, 0.0032	0.0044	0.0053, 0.0064, 0.0032	0.0044
p (mm)	–	–	23, 45, 68	40
ΔT_{sub} (°C)	0–20			
P_{in} (kPa)	740			

[a] A total of six capillary lengths, viz., 6.4 m, 5.6 m, 4.8 m, 4.0 m, 3.2 m, 2.4 m, have been used for each test-section.

The uncertainty in the measurement of capillary tube diameters was 0.01 mm, capillary tube lengths 0.1 mm and surface roughness is 0.01 μm. Similarly, uncertainties in the measurement of pressure was 3.5 kPa in case of pressure gauges and 0.25% full scale (2.6 kPa) in case of pressure transducers while uncertainty in the measurement of temperature using T-type thermocouple was 0.1 °C. The uncertainty in the measurement of mass flow rate was 1% full scale (0.5 kg h^{-1}). All the instruments were calibrated prior to installation.

3. Results and discussion

First of all, a comparison of experimental results of straight capillary tube with the correlation of Melo et al. (1999) has been made to check the integrity of the experimental set-up. Melo et al. (1999) correlation for mass flow rate of R-134a is given below:

$$\pi_5 = 0.125\pi_1^{0.460}\pi_2^{0.552}\pi_3^{0.178}. \quad (2)$$

A comparison of experimental results of straight capillary tube has been made with those predicted by the widely accepted Melo et al. (1999) correlation to establish the integrity of present experimental set-up. Fig. 4 has been drawn taking measured experimental refrigerant mass flow rate in a straight capillary tube as abscissa and that predicted by Melo et al. (1999) correlation for the present experimental input conditions as ordinate. It has been found that Melo et al. (1999) correlation overpredicts the experimental data of both *instrumented* (with pressure taps) and *non-instrumented* (without pressure taps) straight capillary tubes in an error band of 0 to +20%. Further, more than 75% data are in agreement with Melo et al. (1999) correlation in the error band of 0 to +15%. It is to be noted that Melo et al. (1999) correlation has predicted their own experimental data in an error band of ±15%. Therefore, it can be concluded that the data acquired from the present experimental set-up are in good agreement with predictions of Melo et al. (1999) correlation. This establishes the integrity of experimental set-up.

In order to show the effect of pressure taps on the mass flow rate, the results of straight and spiral capillary instrumented and non-instrumented capillary tubes have been shown in fig. 5. It is observed that the provision of taps for the measurement of pressure does not have any significant effect on the mass flow rate through the capillary tube as the deviation in mass flow rate in instrumented is less than 1%. The uncertainty in the refrigerant flow measurement is also 1%. Therefore, any conclusion regarding the effect of pressure taps on the refrigerant mass flow rate cannot be drawn. The insignificant effect of pressure taps on mass flow rate is due to the fact that the pressure tap area is very small in comparison to the internal surface area of the capillary tube and the flow passes near the taps almost undisturbed as a flexible boundary is formed at the location of tap as the refrigerant in the lines connecting taps to pressure header is stagnant.

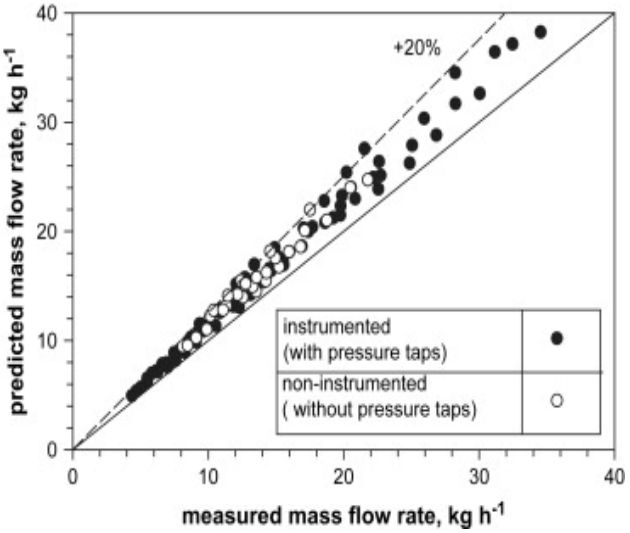

Fig. 4. Comparison of mass flow rate predicted by Melo et al. (1999) correlation with the measured mass flow rate.

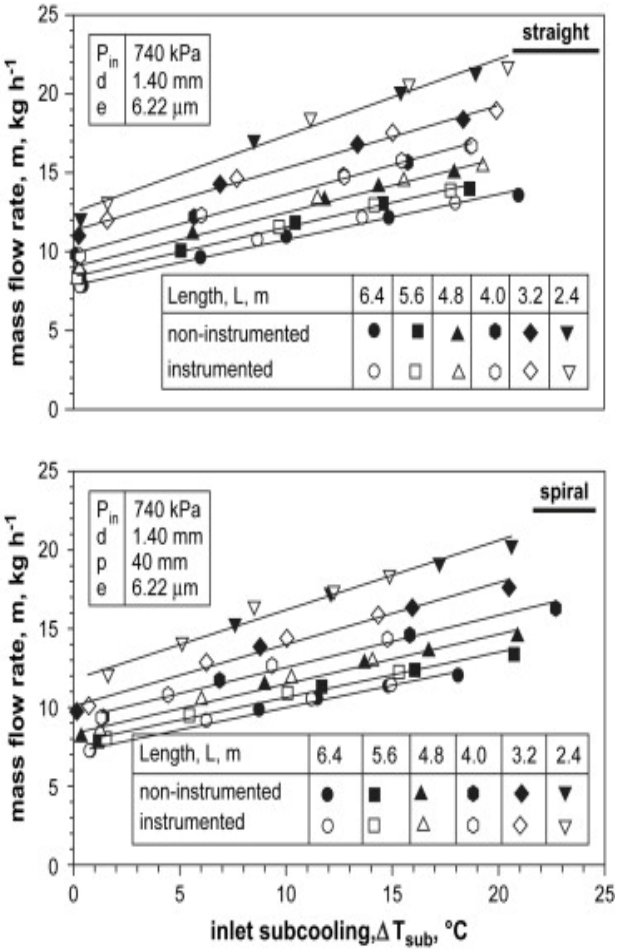

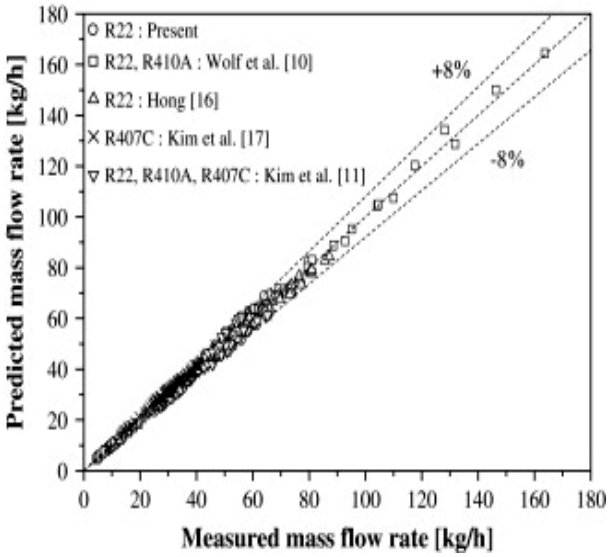

Fig. 5. Comparison of the mass flow rate for straight and coiled instrumented and non-instrumented capillary tubes.

The database of the present correlation was obtained from the experimental data for the straight capillary tubes obtained from the literature and the present data for the coiled capillary tubes. The data for the straight capillary tubes formed the basis for determining the relationship between the mass flow rate and capillary geometry (L and d), operating conditions, and refrigerant properties. The present data mainly covered the effects of the coiled shape on the mass flow rate.

Table 2 shows the detailed information on the present database including data source and number of data points. The database contains a total of 364 data points for R22, R410A, and R407C. The database covered capillary tube diameters from 0.96 mm to 2.3 mm, capillary tube lengths from 508 mm to 2032 mm, upstream pressures from 1445 to 2890 kPa, and inlet subcoolings from 1.5 to 30 °C. The ranges of these values will impose limitations on the application of the correlation.

Table 2
The database of the present correlation

Items	Present	Wolf et al.	Kim et al.	Hong	Kim et al.
Length [mm]	1000	508–2032	1000	1000–2000	700–1300
Diameter [mm]	1.2–1.5	1.3–2.3	1.2–2.0	1.1–1.7	0.96–1.36
Condensing pressure [kPa]	1553–2152	1445–2890	1534–1943	1439–1930	1666–2336
Subcooling [°C]	3.5–11.5	3–30	1.5–10	3–18	0.7–14.1
Refrigerant	R22	R22, R410A	R22, R407C, R410A	R22, R407C	R407C
No. of data point	90	76	36	53	109
Capillary shape	Coiled/straight	Straight	Coiled/straight	Straight	Straight

Since, cut-and-try method has been employed to carry out the investigation, for each cut of length, the corresponding mass flow rate has been recorded for different inlet sub-cooling. Fig. 6 has been drawn with length of capillary as abscissa and refrigerant mass flow rate as ordinate for the inlet sub-cooling of refrigerant being in the range of 0–0.5 °C. For the sake of comparison the straight tube data have also been plotted. The refrigerant mass flow rate rises with the increase in coil pitch and becomes highest for straight capillary tube. The best fit lines for straight and 20 mm pitch spiral capillary tubes have been drawn to quantify the effect of coiling. It has been observed that the mass flow rate is reduced in the range of 5–10% for all lengths of capillary tube. In fact, the coiling effect is pronounced for higher capillary tube diameters. The reason for the increase in mass flow rate with the increasing coil pitch is that increasing pitch leads to straightening of the capillary tube. The mass flow rate is highest for straight capillary tube as the straight capillary tube offers least resistance to the refrigerant flow. Further, it can be seen from the figure that the refrigerant mass flow rate increases with reduction in capillary tube length, i.e., when the length is reduced from 6.4 m to 2.4 m, the mass flow rate is increased by 45%, 55% and 60% for tube diameters of 1.12 mm, 1.40 mm and 1.63 mm, respectively. Also, the mass flow rate increases tremendously with the small increase in tube diameter, i.e., as the tube diameter is increased from 1.12 mm to 1.63 mm, the mass flow is increased by 150% and 180% for capillary lengths of 6.4 m and 2.4 m, respectively. As per Darcy–Weisbach equation for pipe flow (Douglas et al., 1995), the pressure drop in a pipe is directly proportional to pipe length and inversely proportional to fifth power of pipe diameter. This fact also finds agreement with the experimental results.

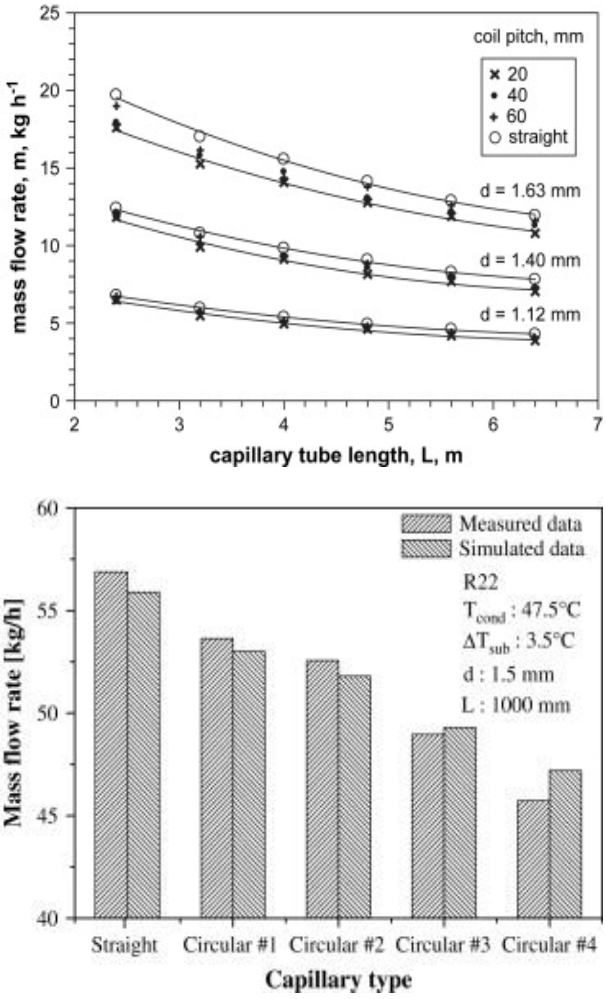

Fig. 6. Effect of coil pitch and capillary tube length on refrigerant mass flow rate.

The cumulative effect of coil pitch, capillary tube diameter, the inlet subcooling and capillary tube length on the refrigerant mass flow rate has been presented in fig. 7. It can be observed that with a slight increase in capillary tube diameter, the refrigerant mass flow rate increases drastically. At 10 °C inlet subcooling, when the diameter is increased from 1.12 mm to 1.63 mm the refrigerant mass flow rate is increased in range of 170 ± 5% for all capillary tube lengths. At the same inlet subcooling of 10 °C, as the capillary length is reduced from 6.4 m to 2.4 m, the refrigerant mass flow rate is increased in the range of 50 ± 5% for all tube diameters. Similarly, if the inlet subcooling is increased from 0 °C to 10 °C, the refrigerant mass flow rate is increased in a range 45 ± 2% for all capillary tube diameters, lengths and pitches. In fact, the length of liquid region increases with the rise in inlet subcooling. Since the pressure drop is less in liquid region as compared to that in the two-phase region, the refrigerant mass flow rate increases with the rise in inlet subcooling. The refrigerant mass flow rate also increases with the coil pitch. It has been observed that lower the pitch lesser will be the refrigerant mass flow rate. For 10 °C inlet subcooling, the refrigerant mass flow rate for 20 mm, 40 mm and 60 mm spiral capillary tubes in comparison to the straight capillary tube is reduced in a range of 5–15%. This is due to the fact that friction factor decreases with the increase in coil pitch and is least for the straight tube. Furthermore, increasing the coil pitch reduces the curvature thereby decreasing the resistance to the refrigerant flow.

All the available correlations in the literature are mostly derived for straight capillary tubes. The mass flow rate of refrigerant through the adiabatic spiral capillary tube depends upon the capillary tube diameter, length, coil pitch, roughness and the inlet subcooling. As the capillary tubes are available in a limited band of roughness, the roughness effect is ignored in the development of correlation. Therefore, the roughness is not considered in the development of the correlation. Other parameters like inlet pressure, the density, the viscosity and specific heat of the refrigerant have also an influence on the mass flow rate. The REFPROP 7.0 database (McLinden et al., 2002), has been used to determine the thermodynamic and transport properties of the refrigerant R-134a, appearing in eq. (3). The mass flow rate can be represented as a function of all these parameters.

$$m=f_1(P_{\text{in}},L,d,p,\Delta T_{\text{sub}},\rho_{\text{f}},\mu_{\text{f}},c_p). \quad (3)$$

In the above equation, the total number of variables is nine ($N = 9$), out of which four variables, viz., d, ρ_{f}, μ_{f} and c_p are fixed as repeating variables, i.e. ($M = 4$). Buckingham-π theorem (Douglas et al., 1995) states that the number of non-dimensional π-terms will be the difference between the total number of parameters and the number of repeating variables, i.e. ($N - M = 5$). By performing the dimensional analysis, all the five π-terms and uncertainties associated with each π-term have been mentioned in table 3.

Table 3
Non-dimensional parameters

π-Group	Definition	Description	Relative uncertainty $\frac{\delta\pi}{\pi}$
π_1	$\frac{d^2 p_f P_{in}}{\mu_f^2}$	Inlet pressure	0.0176
π_2	$\frac{L}{d}$	Geometry effect	0.1564
π_3	$\frac{d^2 p_f^2 c_p \Delta T_{sub}}{\mu_f^2}$	Inlet subcooling	0.0186
π_4	$\frac{P}{d}$	Effect of coiling	0.0071
π_5	$\frac{m}{d\mu_f}$	Mass flow rate	0.0133

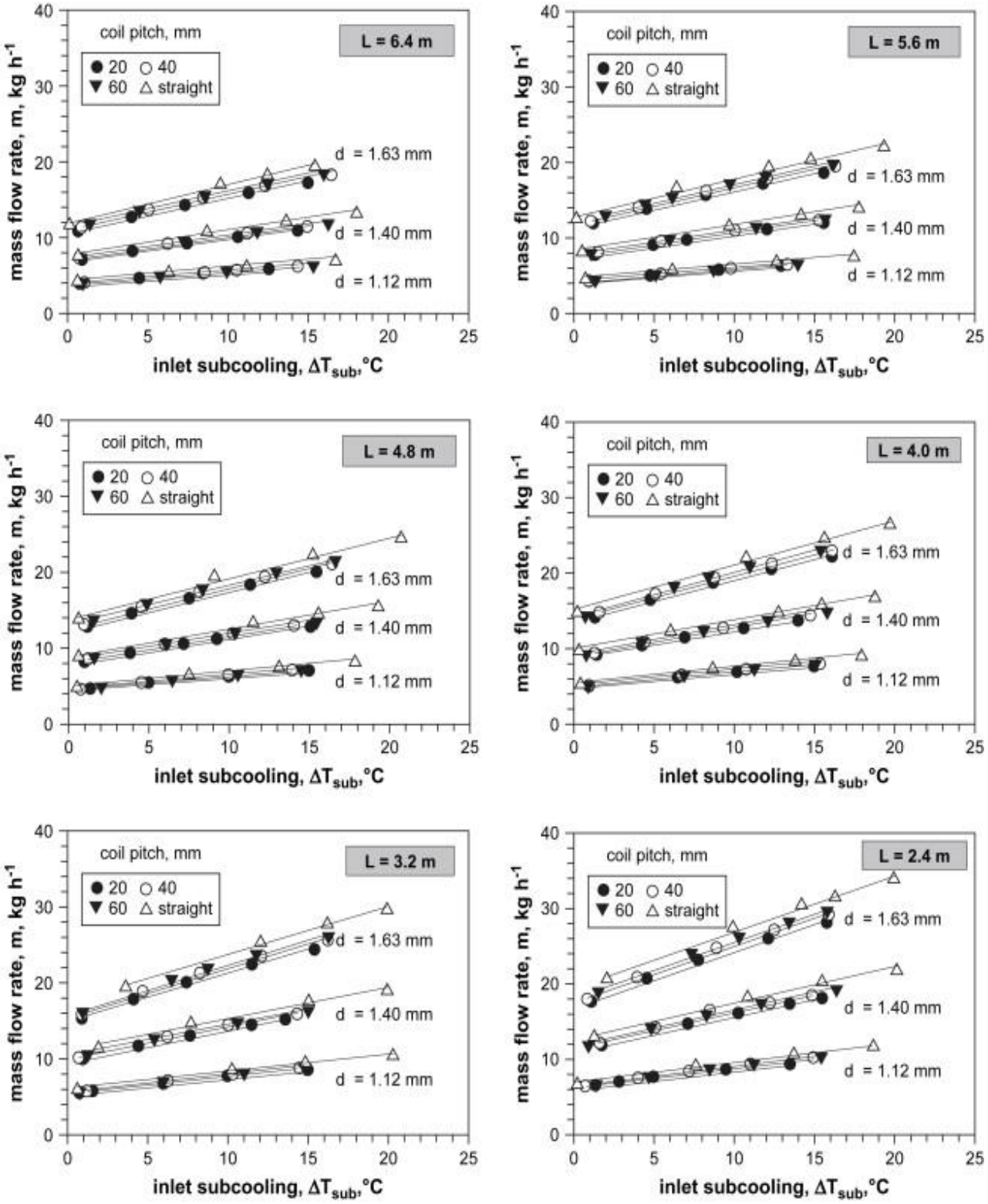

Fig. 7. Variation of mass flow rate with capillary length, diameter, pitch and inlet subcooling.

Eq. (3) in non-dimensional form can be represented as follows:

$$\pi_5 = f_2(\pi_1, \pi_2, \pi_3, \pi_4). \quad (4)$$

Eq. (4) can be further expressed in a non-linear power law form as

$$\pi_5 = C\pi_1^{c_1}, \pi_2^{c_2}, \pi_3^{c_3} F, \quad (5)$$

where C is a constant and F is the coiling factor.Regression analysis of 275 data sets of coiled capillary tube and 103 data sets of straight capillary tube has resulted into the following correlation:

$$\pi_5 = C\pi_1^{0.464}, \pi_2^{-0.503}, \quad (6)$$

For straight capillary tube $C = 0.4587$, $F = 1$ and for spiral capillary tube $C = 0.2607$ and

$$F = \pi_4^{0.0393}.$$

4. Correlation development

A dimensionless correlation was developed to predict refrigerant mass flow rate with the straight and the coiled capillary tubes. Operating parameters considered in this study were inlet pressure P_{in}, subcooling ΔT_{sub}, and saturation pressure P_{sat} corresponding to inlet temperature. The pressure difference $P_{in} - P_{sat}$ showed strong influence on the refrigerant mass flow rate through the capillary tube because it determined the length of the liquid portion in the capillary tube. The effects of metastable flow and friction were considered by including dynamic viscosity μ and densities ρ of both the liquid and vapor phases, and surface tension σ and. The dynamic viscosity μ and the density ρ were replaced by kinematic viscosity υ to reduce the number of π groups because the kinematic viscosity υ is μ/ρ. The critical temperature T_c and heat of vaporization h_{fg} were included to non-dimensionalize the inlet subcooling ΔT_{sub} and to consider the potential effects of vapor bubble formation and growth, respectively. The effects of outlet pressure were neglected since choking flow conditions were easily established in capillary tubes for typical steady-state applications. The surface roughness was not included in the present correlation because the commercial capillary tubes were available only in a limited band of surface roughness.

As given in eq. (5), the capillary equivalent length L_e was introduced into the present correlation to reflect the flow characteristics in the coiled capillary tubes. Capillary tube diameter d and length L were also included in the correlation to consider capillary size effects. In addition, the coil diameter D and semi-circumference numbers of coiled tubes n were incorporated into the capillary equivalent length L_e to explain the effects of the coiled shape.

The refrigerant mass flow rate through coiled capillary tubes can be represented by eq. (6) in functional form by combining all of these variables:

Seven dimensionless π-groups were derived by combining selected variables in eq. (7) based on the Buckingham π-theorem. The definition and effects of each π-group on capillary tube flow are given in table 3. The coefficient and exponents of the independent π-groups were determined by using a non-linear regression technique with the present database. All properties of the refrigerants were calculated by using. The generalized correlation for refrigerant mass flow rates through coiled capillary tubes. In order to compare the predicted mass flow rate by the proposed correlation with the measured mass flow rate, fig. 8 has been drawn. The mass flow rate predicted by eq. (6) is in good agreement with the experimental mass flow rate as 85% of the straight capillary tube mass flow rate data lies in an error band of ±10%. While, in case of coiled tube the same correlation predicts 90% of the mass flow rate in the error band of ±10%.

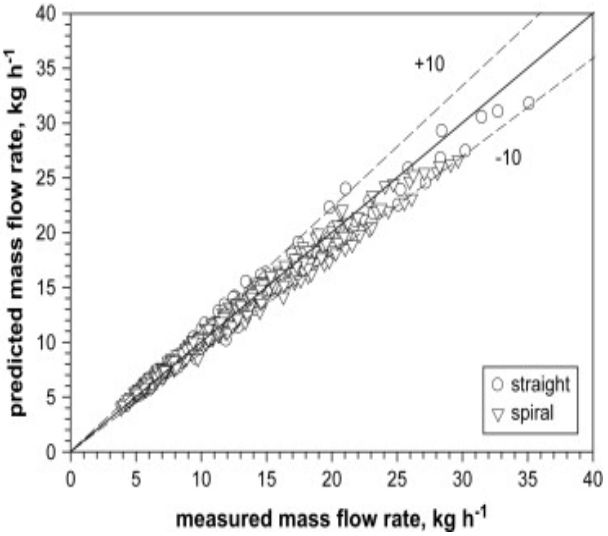

Fig. 8. Comparison of the predicted mass flow rate with the measured experimental mass flow rate.

In fig. 9, the proposed correlation for straight capillary tube has been compared with already established correlations of Melo et al. (1999) and Wolf et al. (1995). Melo et al. (1999) correlation has already been shown in eq. (2). Wolf et al. (1995) correlation for R-134a (30 data sets) with ±5% agreement with their own experimental data given by

$$\pi_5 = 0.0129(\pi_1)^{0.492}(\pi_2)^{-0.387}(\pi_3)^{0.187}. \quad (7)$$

The percentage deviation appearing in fig. 9 is evaluated using the following equation:

$$\textit{percentage deviation} = \frac{m_{predicted} - m_{measured}}{m_{measured}} 100 \, . \quad (8)$$

Fig. 9 shows the deviation of mass flow rates predicted by Melo et al. (1999) correlation, Wolf et al. (1995) correlation and the proposed correlation from the measured experimental mass flow rate. The refrigerant mass flow rate predicted by Melo et al. (1999) correlation lies in the error band of 0 to +20%. Melo et al. (1999) correlation has been developed for range of operating parameters different from the present experimental investigation. The range of tube diameter for Melo et al. (1999) correlation is 0.66–1.05 mm while in the present case it is 1.12–1.63 mm, range of length is 1.99–3.02 m while in this case it is 2.4–6.4 m and range of inlet subcooling is 0–16 °C, whereas, for the present case it is 0–25 °C. The range of inlet pressure for Melo et al. (1999) correlation is 900 kPa and 1100 kPa while in the present study the inlet pressure has been kept nearly constant at 740 kPa. Most importantly it is the internal tube roughness, which is really making this difference. The capillary tube internal tube roughness as used by Melo et al. (1999) experiments lies in the range of 0.7–1.1 μm, whereas, in the present case the roughness is in the range of 3.5–7.1 μm was in the tube. Therefore, with such a large difference in the range of operating parameters overprediction of 5% is a fairly good proposition. Also, the present experimental investigation has been carried out on both instrumented and non-instrumented straight capillary tubes whereas Melo et al. (1999) correlation has been developed for non-instrumented straight capillary tube.

On the other hand Wolf et al. (1995) correlation predicts the same in the error band of +10 to +38%. Such a large discrepancy may be because of the fact that Wolf et al. (1995) has been developed for four different refrigerants R-134a, R-22, R-410a and R-152a with only 30 data points of R-134a used in the development of Wolf et al. (1995) correlation.

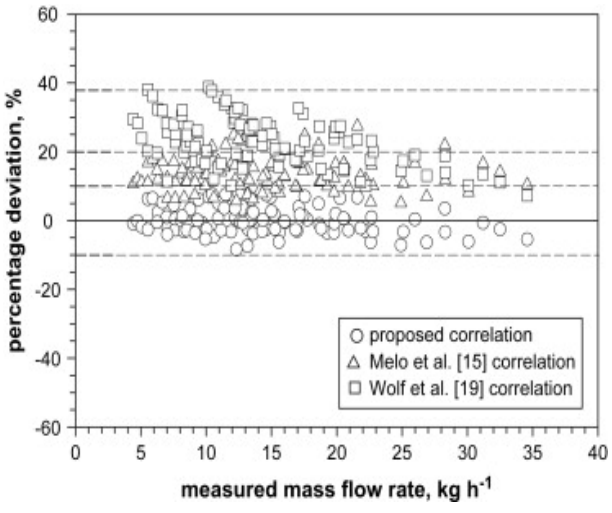

Fig. 9. Comparison of the proposed correlation with Melo et al. (1999) and correlations.

5. Conclusions

The performance of straight and coiled capillary tubes with R22 was measured as the operating conditions, tube geometries, and coiled shape were varied. The mass flow rates of the coiled capillary tubes decreased by 5–16% more than those of the straight capillary tubes under the same operating conditions due to increased flow friction resulting from strong coiled effects. These results were confirmed by numerical simulation of the performance of the coiled capillary tubes. A generalized correlation to predict the refrigerant mass flow rate through both straight and capillary tubes was derived by implementing dimensionless parameters that were generated using the Buckingham π-theorem considering the effects of tube inlet conditions, coiled tube geometries, and refrigerant properties. The coiled effects of the coiled capillary tube were considered by introducing the capillary equivalent length L_e. The relative deviations of the predictions of the present correlation from the present database for R22, R410A, and R407C were between −8.3% and 8.8%. In addition, the average and standard deviations of the present correlation were 0.24% and 4.4%, respectively.

Nomenclature

c_p	specific heat at constant pressure (J kg^{-1} K^{-1}),
D	coil diameter (m),
De	Dean number,
d	capillary tube internal diameter (m),
ΔT_{sub}	degree of sub-cooling (°C),
e	roughness height (m),
L	capillary tube length (m),
L_e	capillary equivalent length (m),
M	number of repeating variables,
m	mass flow rate (kg s^{-1}),
N	total number of variables,
n	semi-circumference numbers of coiled tubes,
P	pressure (kPa),
p	coil pitch (m),
P_{in}	inlet pressure (kPa),
P_c	critical pressure (kPa),
P_{sat}	saturated pressure (kPa),
T	temperature (°C), and
v	specific volume (m^3 kg^{-1}).

Greek letters

μ	viscosity (kg m^{-1} s^{-1}),
ε	absolute roughness (mm),
υ	kinematic viscosity (m^2/s),
σ	surface tension (N/m), and
ρ	density (kg m^{-3}).

Subscripts

cond	condenser,
Evap	evaporator,
in	capillary tube inlet, and
f	liquid.

References

[1] H. Ito, "Friction Factors for Turbulent Flow in Curved Pipes", J. Basic Eng., pp. 123–134 (1959).

[2] P.K. Bansal and A.S. Rupasinghe, "An Empirical Correlation for Sizing Capillary Tubes", Int. J. Refrigeration, Vol. 19 (8), pp. 497–505 (1996).

[3] J.M. Choi and Y.C. Kim, "The Effects of Improper Refrigerant Charge on the Performance of a Heat Pump with an Electronic Expansion Valve and Capillary Tube", Energy, Vol. 27 (4), pp. 391–404 (2002).

[4] C. Melo, R.T.S. Ferreira, C.B. Neto, J.M. Goncalves and M.M. Mezavila, "An Experimental Analysis of Adiabatic Capillary Tubes", Appl. Therm. Eng., Vol. 19, pp. 669–694 (1999).

[5] R.R. Bittle and M.B. Pate, "A Theoretical Model for Predicting Adiabatic Capillary Tube Performance with Alternative Refrigerants", ASHRAE Trans., Vol. 102 (2), pp. 52–64 (1996).

[6] N.M. Bolstad and R.C. Jordan, "Theory and Use of the Capillary Tube Expansion Device; Part II, Non-Adiabatic Flow", Refrigerating Eng., Vol. 57 (6), pp. 572–583 (1949).

[7] Z. Yufeng, Z. Guobing, X. Hui and C. Jing, "An Assessment of Friction Factor and Viscosity Correlations for Model Prediction of Refrigerant Flow in

Capillary Tubes", Int. J. Energy Res., Vol. 29, pp. 233–248 (2005).
[8] S.J. Kuehl and V.W. Goldschmidt, Modeling of Steady Flow of R-22 Through Capillary Tubes", ASHRAE Trans., Vol. 97 (1), pp. 139–148 (1991).
[9] H. Ito, "Friction Factors for Turbulent Flow in Curved Pipes", Journal of Basic Engineering D81, pp. 123–134 (1959).
[10] Kuehl and Goldschmidt, S.J. Kuehl and V.W. Goldschmidt, Steady Flows of R-22 through Capillary Tubes: Test Data, ASHRAE Transactions", pp. 719–728 (1990).
[11] S.G. Kim, S.T. Ro and M.S. Kim, "Experimental Investigation of the Performance of R22, R407C and R410A in Several Capillary Tubes for Air-Conditioners", International Journal of Refrigeration, Vol. 25, pp. 521–531(2002).
[12] M.K. Khan, R. Kumar and P.K. Sahoo, "Flow Characteristics of Refrigerants Flowing Inside an Adiabatic Spiral Capillary Tube", HVAC and R Research ASHRAE, Vol. 13 (5), pp. 731–748 (2007).
[13] Mikol, E.P. Mikol, "Adiabatic Single and Two-Phase Flow in Small Bore Tubes", ASHRAE Journal, pp. 75–86 (1963).
[14] Mori and Nakayama, Y. Mori and W. Nakayama, "Study on Forced Convective Heat Transfer in Curved Pipes", (2nd report, turbulent region), International Journal of Heat Mass Transfer, Vol. 10, pp. 37–59 (1967).
[15] C. Melo, R.T.S. Ferreira, C.B. Neto, J.M. Goncalves and M.M. Mezavila, "An Experimental Analysis of Adiabatic Capillary Tube", Applied Thermal Engineering, Vol. 19, pp. 669–684 (1999).
[16] McLinden, M.O., Klein, S.A., Lemmon, E.W., REFPROP-Version 7– Thermodynamic and Transport Properties of Refrigerants and Refrigerant Mixtures. NIST Standard Reference Database (2002).
[17] C. Park, S. Lee, H. Kang and Y. Kim, "Experimentation and Modeling of Refrigerant Flow through Coiled Capillary Tube", International Journal of Refrigeration, Vol. 30, pp. 1168–1175 (2007).
[18] G. Valladares, "Numerical Simulation and Experimental Validation of Coiled Adiabatic Capillary Tubes", Applied Thermal Engineering, Vol. 27, pp. 1062–1071 (2007).
[19] D.A. Wolf, R.R. Bittle, M.B. Pate, "Adiabatic Capillary Tube Performance with Alternative Refrigerants", ASHRAE Research Project RP-762 (1995).
[20] G. Zhou and Y. Zhang, "Numerical and Experimental Investigations on the Performance of Coiled Adiabatic Capillary Tube", Applied Thermal Engineering, Vol. 26, pp. 1106–1114 (2006).
[21] G. Zhou and Y. Zhang, "Experimental Investigation on Hysteresis Effect of Refrigerant Flowing Through a Coiled Adiabatic Capillary Tube", Energy Conversion and Management, Vol. 47, pp. 3084–3093 (2006).

Received August 19, 2008
Accepted January 28, 2008